Wnt signalling mediated by Tbx2b regulates cell migration during formation of the neural plate

Steven H. Fong[1,*], Alexander Emelyanov[1,*], Cathleen Teh[1] and Vladimir Korzh[1,2,†]

[1]Institute of Molecular and Cell Biology, 61 Biopolis Drive, Proteos, 138673 Singapore
[2]Department of Biological Sciences, National University of Singapore, 10 Kent Ridge Crescent, 119260 Singapore
*These authors contributed equally to this work
†Author for correspondence (e-mail: vlad@imcb.a-star.edu.sg)

Accepted 9 June 2005

Development 132, 3587-3596
Published by The Company of Biologists 2005
doi:10.1242/dev.01933

Summary

During gastrulation, optimal adhesion and receptivity to signalling cues are essential for cells to acquire new positions and identities via coordinated cell movements. T-box transcription factors and the Wnt signalling pathways are known to play important roles in these processes. Zebrafish *tbx2b*, a member of the TBX2 family, has previously been shown to be required for the specification of midline mesoderm. We show here that *tbx2b* transcripts are present during mid-gastrula before its expression is detected by whole-mount in situ hybridization. Isolated ectodermal cells deficient in Tbx2b have altered cell surface properties and the level of cadherins in these cells is lower. In chimaeric embryos generated by cell transplantation and single blastomere injections, Tbx2b-deficient cells are defective in cell movement in a cell-autonomous manner, resulting in their exclusion from the developing neural plate. Using this 'exclusion' phenotype as a screen, we show that Tbx2b acts within the context of Fz7 signalling. The exclusion of cells lacking T-box proteins in chimeras during development was demonstrated with other T-box genes and may indicate a general functional mechanism for T-box proteins.

Key words: T-box, Cell adhesion, Zebrafish, Frizzled 7, Dishevelled, DIX domain, β-catenin

Introduction

During gastrulation, concurrent cell movement and cell fate specification eventually lead to the formation of germ layers and axes in the embryo. Because zebrafish embryonic cells are pluripotent up to the early gastrula stages (Ho and Kimmel, 1993), alteration of cell movement can cause changes in fate specification by virtue of exposure to local signalling cues prevalent in the 'adopted' position. Conversely, a failure in fate specification can lead to changes in cell movement behaviour.

In the zebrafish ectoderm, individual cells lose their independence and integrate their behaviour to achieve a coherent movement over the yolk as a sheet (Concha and Adams, 1998), while the underlying mesodermal cells migrate as individuals or groups of cells. This is in contrast to *Xenopus*, where the ectoderm is tightly coupled to the mesoderm (Shih and Keller, 1994). Optimal cell adhesion is essential for proper cell movement (Nelson and Nusse, 2004). Cell-surface adhesion molecules such as cadherins control cell-cell adhesion and influence cell migration. Disparity in cell adhesion properties among neighbouring cells is known to lead to loss of integrity and cell sorting within the ectodermal sheet (Concha and Adams, 1998).

The embryonic ectoderm has the potential to acquire either epidermal or neural fates. According to the default model, neural induction depends on the suppression of bone morphogenetic protein (Bmp, vertebrate homologue of Dpp) signalling by organizer-derived inhibitors (Munoz-Sanjuan and Brivanlou, 2002). Mass cell movements during gastrulation, especially that of convergent extension (CE), eventually establish the neural plate, which can be differentiated from the remaining epidermal ectoderm by early neural markers such as *sox19* (Vriz and Lovell-Badge, 1995). CE movement is most extensively investigated at the molecular level within the context of mesoderm formation (Myers et al., 2002). As such, the molecular mechanism governing dorsal movement of the overlying ectoderm leading to the formation of the neural plate is not well understood.

In *Xenopus*, Wnt/β-catenin has been demonstrated to inhibit Bmp (Baker et al., 1999) and is required for the expression of secreted Bmp antagonists (Wessely et al., 2001). In the zebrafish, Wnt/β-catenin-dependent *bozozok* (*boz*) is sufficient to suppress expression of *bmp* (Fekany-Lee et al., 2000). This is consistent with the role of β-catenin-dependent Wnt signalling, or canonical Wnt signalling, in fate determination (Moon et al., 2002). β-Catenin-independent Wnt signalling, or non-canonical Wnt signalling, has been demonstrated to influence morphogenetic cell movement (Tada et al., 2000; Heisenberg et al., 2000) by controlling Dishevelled (Ds)-mediated polarity in a manner reminiscent of the *Drosophila* planar-cell-polarity (PCP) pathway. However, in addition to its function in the Wnt signalling pathway, β-catenin also binds to the cytoplasmic domain of type 1 cadherins and plays an essential role in the structural organization and function of cadherins in the actin cytoskeleton (Jamora et al., 2003). Different cadherins have been shown to stimulate directly the

differentiation of stem cells into specific tissues (Larue et al., 1996). As such, there is a possible convergence of Wnt, β-catenin and cadherin signalling in adhesion, morphogenetic movement and differentiation.

Transcription factors of the T-box family (Tbx) play important roles in vertebrate development (Smith, 1999; Wilson and Conlon, 2002). *Brachyury* (*T*) and the zebrafish orthologue *no tail* (*ntl*) are known to be essential for the specification of axial mesoderm (Smith, 1999). In addition, *T*, *Tbx16*/*spadetail* (*spt*) and *Xbra* have been shown to be required for mesodermal cell movement (Wilson and Beddington, 1997; Ho and Kane, 1990; Kwan and Kirschner, 2003). A number of human disorders have been linked to mutations in T-box genes, confirming their medical importance (Packham and Brook, 2003). Recently, a knockout of TBX2 in mice resulted in abnormal development of the heart (Harrelson et al., 2004).

Ntl is shown to function in parallel to Wnt5 signalling in the morphogenesis of the posterior body (Marlow et al., 2004) and Xbra is shown to regulate Wnt11 expression during gastrulation (Tada and Smith, 2000). The *Drosophila Tbx2*-related opto-motor blind (omb) is regulated by the Wingless (Wg), Decapentaplegic (Dpp) (Grimm and Pflugfelder, 1996) and Hedgehog (Hh) (Kopp and Duncan, 1997) signalling pathways; *Xenopus* Tbx2 is known to function within the Sonic hedgehog (Shh) pathway (Takabatake et al., 2002); in chick, Tbx2 is known to function through both Shh and Bmp signalling (Suzuki et al., 2004).

Zebrafish *tbx2b* was previously named *tbx-c*. Using a dominant-negative (dn) approach, it was shown to function downstream of Tgfβ signalling, of *ntl* and of *floating head* (*flh*) in the late-phase specification of the notochord and development of motoneurons (Dheen et al., 1999). In this report, we show that neural development is dependent on early Tbx2b activity during gastrulation. Using a combination of antisense morpholino oligonucleotide (MO) gene 'knockdown' (Nasevicius and Ekker, 2000) and in vivo analysis of chimaeric embryos generated by cell transplantation or single blastomere injection, we demonstrate that, during neural plate formation and neuronal specification, Tbx2b functions within the context of Wnt signalling to mediate cell migration.

Materials and methods

Reagents

MOs were obtained from Gene Tools (USA). Sequences were as follows (sequence complementary to predicted start codon is underlined): *tbx2b* MO, 5′-GGA AAG GGT GGT AAG CCA TCA CAG T-3′; *tbx2b* MOv2, used for all data generated in this study, 5′-GGT AAG CCA TCA CAG TCC CTG TAA A-3′; *fz7* MO, 5′-ATA AAC CAA CAA AAA CCT CCT CGT C-3′; *fz7a* MO, 5′-CCA ATC TGG AGC TCC AGA CGT GAC C-3′; *fz2* MO, 5′-ACA AAA TGA GTC CGG CAA ACT ATG C-3′; *axin1* MO, 5′-CAT AGT GTC CCT GCA CTC TGT CCC A-3′ phenocopies the mutant *masterblind*; *stbm* MO is as described (Park and Moon, 2002); *ntl* MO is as described (Nasevicius and Ekker, 2000); *b-jun* MO, 5′-ACT CAT AGA GTT GGA AAA CCG GTG G-3′; *c-jun* MO, 5′-TTT AGG CGC TGT TAA GCA CTG TCC G-3′. Stocks (1 mM) were made in Danieau's solution. Pertussis toxin was obtained from Sigma (P2980, 200 mg/ml).

Whole-mount in situ hybridization, immunohistochemistry, western blot and TOP-Flash assay

Whole-mount in situ hybridization and whole-mount immunohistochemistry with anti-fluorescein-POD were performed according to established techniques. Proteins were extracted from 20 embryos/lane for western blot, and detected with chemiluminescent detection kit (Cell Signalling Technology, USA). TOP-flash assay was performed as described (Korinek et al., 1997).

Dominant negative Fz7-EGFP/BAC construct

Dn-*fz7* targeting construct was generated from *fz7* cDNA by replacing the stop codon with an EGFP-kanamycin cassette using overlapping amplicons and primer extension. Primer sequences were as follows: 5′UTRF, 5′-AGG AAA CCG CAC TCT GTT CA-3′; *fz7*R, 5′-TAC CGT CGT CTC GCC CTG GTT-3′; *fz7*EGFPF, 5′-GGC GAG ACG ACG GTA ATG GTG AGC AAG GGC-3′; kanR, 5′-TCA GAA GAA CTC GTC AAG AAG GCG ATA GAA-3′; kan3′UTRF, 5′-CTT CTT GAC GAG TTC TTC TGA GAA AAA GAG CGA TCG TTT TCG-3′; and 3′UTRR, 5′-ACA AGT CCC CGG TTA AAA CAA GTG TTG G-3′. The resultant dn*fz7*-EGFP construct was co-transformed with pGETrec into *E. coli* DH10B carrying a BAC of the intronless *fz7* gene. Homologous recombination was then induced (Narayanan et al., 1999).

Transplantation

Donor embryos were injected at the one-cell stage with fluorescein dextran pre-mixed with MO or Danieau's solution. About 20 cells from each donor were transplanted into wild-type host embryo of the same stage. Chimaeric embryos were grown to 10 and 24 hpf. Location of transplanted cells at 10 hpf was visualized by a combination of immunohistochemistry with anti-fluorescein-POD and *sox19* whole-mount in situ hybridization. Images were taken using the Olympus AX70 (Olympus, Japan) microsope fitted with CCD camera. Fluorescent and bright-field images were superimposed with Photoshop 5.5 (Adobe) software.

Injections at 16 cell stage

Dechorionated 16-cell stage embryos were transferred to a Petri dish with moulded agar (1.5% agarose in egg water) injection wells and one central blastomere was injected with not more than 200 pl of reagents. Injected embryos were allowed to develop to 4 hpf, and then were inspected under a UV dissecting microscope. Embryos with labelled clones in the centre of the blasdoderm, when viewed from the animal pole, that represented a perfect cone when viewed from the side, were allowed to develop further. In this way only ectodermal derivatives were labelled.

Real time RT-PCR

Total DNA-free RNA (1 mg) was subjected to oligo(dT)15 primed RT with PowerScript Reverse Transcriptase (Clontech) according to the manufacturer's recommendations, and 1/20 of the reaction mix was used for PCR. Real-time semi-quantitative PCR assay was carried out using gene-specific primers for *tbx2b* (forward, 5′-AGG AAC CCG TTC TTG AGC AGC-3′; reverse, 5′-AGG CCG CTT GGC AAT CCG GTG-3′), EF1α (forward, 5′-AGA CTG GTG TCC TCA AGCC TG-3′; reverse, 5′-TGA AGT TGG CAG CCT CCA TGG-3′) and *fz7* (forward, 5′-TCA CTG TGG CTC TAC AAA CGA CC-3′; reverse, 5′-TGC ACT TCG AGA CCG GCG TCC-3′) in a DNA Engine Opticon System (MJ Research, USA). SYBR Green was used as the reporter for real-time PCR. Briefly, HotStart Taq (Qiagen) activation for 15 minutes, four segment amplification and quantification program repeated 35 times [95°C for 30 seconds; 62°C for 10 seconds with a single fluorescence measurement; 72°C for 30 seconds, melting curve program (78°C to 95°C)]. Serial dilutions of cDNA were used as standards for semi-quantitation. Correction for inefficiencies in RNA input or reverse transcriptase was performed by normalizing to EF1α

amplification. The comparative C(T) method, calculating relative expression levels compared to control, was used for quantification.

Hanging-drop culture

Hanging-drop cultures were carried out with animal caps from embryos at 50% epiboly as previously described (Steinberg and Takeichi, 1994). Fluorescent images were obtained with a Zeiss Axioplan2 equipped with Zeiss AxioCam HRc CCD camera (Zeiss, Germany).

Results

RT-PCR showed that *tbx2b* transcripts are not maternally supplied and appear only at 50% epiboly (5.5 hpf, Fig. 1A and data not shown). Real-time PCR measurements of the level of transcripts in the dorsal and ventral half of 5.5 hpf embryos (when the shield could be seen with confidence) indicated that *tbx2b* is present at a higher level in the ventral blastoderm than the dorsal blastoderm (Fig. 1E). By 8 hpf and later, the transcripts accumulate in the dorsal blastoderm and dorsal structures – the notochord and neural derivatives (Dheen et al., 1999). This shift in the distribution of *tbx2b* from ventral to dorsal coincides with the dorsal CE movement of cells during gastrulation.

The initial functional analysis on the role of *tbx2b* in development was performed with a dn-Tbx2b lacking the C-terminal transactivation domain (Dheen et al., 1999). For this study, a MO-mediated loss-of-function approach (targeted gene 'knockdown') was adopted. Two anti-*tbx2b* MOs were designed (see Materials and methods). Both straddle the start codon of *tbx2b*, but offset by 10 bases along the 5′-UTR. To establish their efficacy, the two MOs were injected into one-cell stage embryos (pan-embryonic injection). At the same concentration, *tbx2b* MOv2 was more effective in producing a phenotype than *tbx2b* MOv1 and was used for all experiments in this study (henceforth referred to as *tbx2b* MO).

When co-injected with *tbx2b* MO pan-embryonically, translation of a *myc*-tagged *tbx2b* containing the target site for *tbx2b* MO was blocked in a dose-dependent manner (Fig. 1B). The midline axial mesoderm of the morphants, as analyzed and compared with embryos obtained from overexpression of dn-Tbx2b with the marker *sonic hedgehog* (*shh*), had malformed notochord and lacked the floor plate (Fig. 1C). In the most severely affected morphants, only remnants of the notochord were present (Fig. 1D). This is reminiscent of the mutant *flh*, and is in agreement with our previous study (Dheen et al., 1999). These results suggest that the phenotype observed with *tbx2b* MO was indeed specific to the 'knockdown' of *tbx2b*.

Pan-embryonic 'knockdown' of *tbx2b* with *tbx2b* MO delayed the onset and progression of gastrulation by up to 2 hours and produced phenotypes at 24 hpf in a dose-dependent manner. In its most severe form (at 1 pmol/embryo), *tbx2b* morphants display phenotypes similar to *boz*$^{-/-}$ embryos (Fekany-Lee et al., 2000) – short AP axis, absent or malformed notochord, fused somites, small and/or cyclopic eyes, and small brain (Fig. 1F-G). Cross-sections of the morphants at the level of the eyes showed that the neural tube was severely malformed: the ventricle was absent and the eyes were underdeveloped (Fig. 1H,I). Injections of a sense MO up to 10 pmol showed no phenotype.

The disorganized forebrain of the *tbx2b* morphant supported a role for Tbx2b in neural development. However, the severity of the malformation rendered analyses of pan-embryonic morphants ambiguous. To circumvent this, we analyzed the behaviour of Tbx2b-deficient cells in chimaeric embryos. The chimaeras were generated by two complementary approaches aiming to target ectodermal derivatives – cell transplantation and single-blastomere injection.

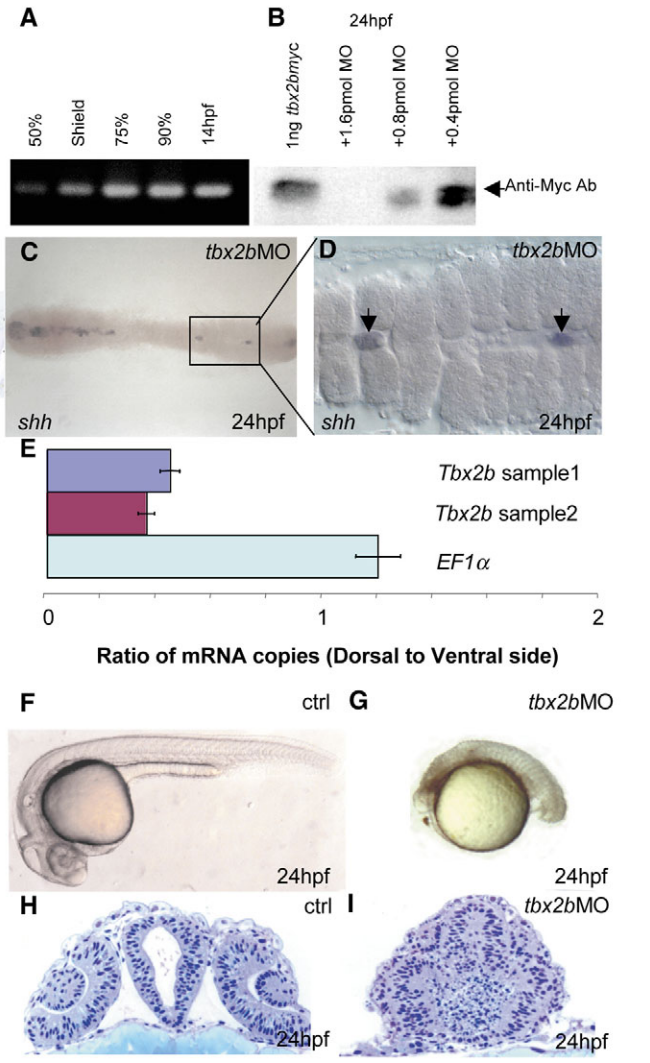

Fig. 1. *tbx2b* MO blocks translation of *tbx2b* and impairs normal development. (A) RT-PCR using primers specific to the 5′-UTR of *tbx2b* shows that this transcript was present as early as 50% epiboly. (B) Western blot with anti-Myc antibody shows that translation of recombinant *tbx2b-myc* was blocked in the presence of *tbx2b* MO in a dose-dependent manner. (C) Dorsal view of *tbx2b* morphant shows the almost complete loss of *shh* in the trunk region of the embryo. The boxed section is enlarged in D, showing the *shh*-positive cells as remnants of notochord (arrow). (E) Real-time PCR shows that *tbx2b* transcripts are present at a higher level in the ventral gastrula (5.5 hpf) when compared with *EF1α*. (F,G) Phenotype of *tbx2b* morphant (2 pmol) (G) when compared with control (F) (see text for description). (H,I) *tbx2b* is required for proper development of the eyes and forebrain. (H) Plastic cross-section through the forebrain of a 24 hpf control embryo at the level of the lens. (I) Cross-section of the *tbx2b* morphant shows severe disorganization of the forebrain and eyes.

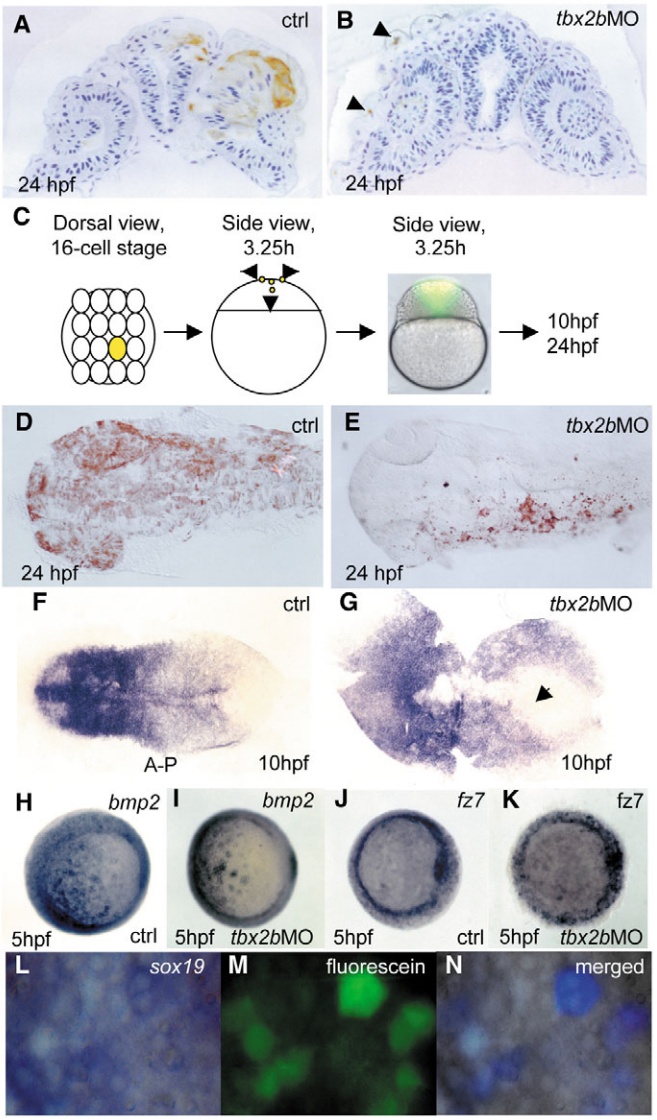

Fig. 2. Tbx2b is required for cells to adopt a neural fate. Deep cells from embryos co-injected with fluorescein-dextran (70 kDa) and *tbx2b* MO at 30% epiboly were transplanted into homochronic wild-type hosts. (A) Cross-section through the neuroretina and brain shows transplanted control labelled cells in the CNS. By contrast (B) transplanted Tbx2b-deficient cells were present only in the epidermis (arrowheads). (C) One central blastomere of 16-cell stage embryos was injected with fluorescein either with or without *tbx2b* MO, and embryos were allowed to develop to 24 hpf. Both control and *tbx2b* morphants developed normally and showed a similar distribution of labelled clones in vivo at 3.25 hours. (D) Dorsal view of 24 hpf control embryo shows labelled cells in neural plate and epidermis. (E) *tbx2b* morphant labelled cells were present only in epidermis. (F,G) Whole-mount in situ hybridization with the pan-neural marker *sox19* shows a delay in convergence of the neural plate in *tbx2b* morphant (arrow in G) compared with control (F). (H-K) Whole-mount in situ hybridization with *bmp2* (H,I) and *fz7* (J,K) show similar expression patterns in control and Tbx2b morphant at 5 hpf. (L-N) Transplanted fluorescein labelled Tbx2b-deficient cells continue to express *sox19* in 5 hpf wild-type host. (N) The merged photographs were enhanced in Adobe Photoshop such that only the simultaneous presence of blue (whole-mount in situ hybridization signal) and green (fluorescence) produced a purple signature. Otherwise, cells remain grey.

Fluorescein-dextran-labelled cells of the animal blastoderm were transplanted from 4 hpf wild-type donor embryos into the same location in homosynchronous wild-type hosts. By 24 hpf, labelled cells were found in the brain, eyes and epidermis (Fig. 2A). In similar transplants, when *tbx2b* morphant cells were placed in wild-type hosts, the labelled cells appeared only in the epidermis (Fig. 2B), supporting the suggestion that Tbx2b may be required during the formation of the neural plate. To confirm this, a single central blastomere of 16-cell stage embryos was injected (referred to as a 1/16 injection, Fig. 2C) with fluorescein, either with or without *tbx2b* MO, and the position of the labelled cells determined later. At 3.25 hpf, both control and *tbx2b* MO-injected embryos showed labelled clones in the ectoderm (Fig. 2C), suggesting that right up to this stage there were no discernible behavioural differences between control and *tbx2b* morphant cells. However, at 24 hpf, control embryos had labelled cells in the eyes, epidermis and CNS (Fig. 2D), while *tbx2b* MO injected embryos displayed labelled cells only in the epidermis (Fig. 2E), thus supporting the observations from transplantation experiments.

In both transplantation and single-blastomere injection experiments, there were reduced numbers of Tbx2b morphant cells compared with control. This could arise from an increase in cell death, from a decrease in cell proliferation or from cell loss. Staining of *tbx2b* morphants with Acridine Orange and TUNEL assay showed no significant increase in apoptosis (not shown). We also failed to observe cell loss because of sloughing during gastrulation, although we could not rule out this possibility later in development. Therefore the reduction in cell count was probably the result of impairment in cell proliferation. This is consistent with reports implicating human TBX2 in cell cycle control and oncogenesis (Jacobs et al., 2000; Prince et al., 2004).

sox19 encodes the early pan-neural transcription factor (Vriz and Lovell-Badge, 1995). It is expressed in the neural plate at 10 hpf (Fig. 2F). In *tbx2b* morphants the neural plate was broader, with a pronounced gap in expression around the midline (Fig. 2G, arrow). We asked if this was likely to be due to an early defect in specification, and thus focused on at early patterning. The expression patterns of *bmp2* and *fz7* in control and morphant 5 hpf embryos were similar (Fig. 2H-K), although expression in the morphants appeared to be more punctate than in control embryos. This could be the result of the delayed epiboly in *tbx2b* morphants. In addition, during gastrulation, transplanted donor cells from *tbx2b* morphants continue to express *sox19* in wild-type hosts at 5 hpf (Fig. 2L-N). These results suggest that early fate specification is not affected by the loss of Tbx2b function; instead, dorsal convergence cell movement was delayed in the morphants.

When 1/16 injected embryos were stained for both fluorescein and *sox19* at 10 hpf, control labelled cells were found in the neural plate and epidermis (Fig. 3A). By contrast, Tbx2b morphant cells were excluded from the neural plate (Fig. 3B). This suggested that the lack of labelled cells in the 24 hpf morphants observed in previous experiments was due to the absence of labelled cells in the neural plate at 10 hpf. 1/16 injection of *tbx2b* mRNA led to the appearance of labelled cells with normal morphology at the midline at 10 hpf, and in the notochord at 24 hpf, in about 10% of the injected embryos (n=30, Fig. 3C,D). Although this result is consistent with the role of Tbx2b in the formation of axial mesodermal structures

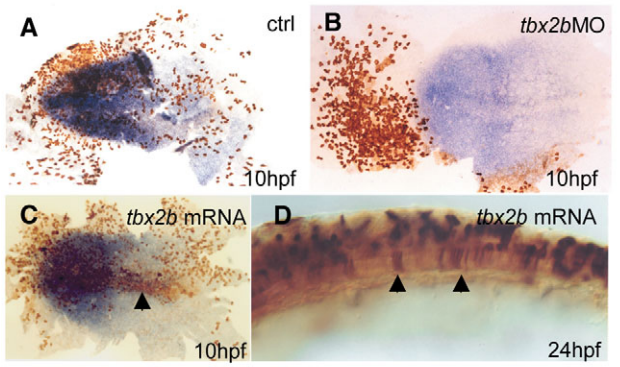

E

Phenotypes / Reagents	Exclusion	No Exclusion	In notochord
Control *n*=50	0%	100%	0
MO(0.05pmol) *n*=38	65%	35%	0
MO(0.05pmol)+ mRNA(0.5ng) *n*=23	61%	39%	0
MO(0.05pmol)+ mRNA(1ng) *n*=22	36%	55%	9% (2)
mRNA(1ng) *n*=30	0%	90%	10% (3)

Fig. 3. 'Exclusion' phenotype can be rescued by *tbx2b* mRNA. Compared with control (A), a 1/16 injection of *tbx2b* MO led to 'exclusion' phenotype (B) at 10 hpf. Neural plate highlighted with *sox19* in blue; fluorescein labelled cells in brown. By contrast, 1/16 injection of *tbx2b* mRNA (1.0 ng) led to (C) labelled cells with normal morphology in the midline (arrow) at 10 hpf and, (D) the notochord (arrows) at 24 hpf, consistent with the role of Tbx2b in axial mesodermal specification. (E) Exclusion phenotype at 10 hpf from *tbx2b* MO (0.05 pmol) was rescued with *tbx2b* mRNA lacking the target site in a dose-dependent manner. In the presence of *tbx2b* MO, 1.0 ng mRNA led to appearance of labelled cells in the midline similar to C and D, while significantly reducing the number of embryos with 'exclusion' phenotype. 0.5 ng mRNA was less effective in reducing the 'exclusion' phenotype but did not cause appearance of labelled cells in the midline.

(Dheen et al., 1999) it is nevertheless interesting and surprising because the clonal population derived from the injected blastomere were ectodermal in origin. This apparent re-specification of fate across germ layers by overexpression of *tbx2b* needs to be further investigated.

The percentage of embryos with an 'exclusion' phenotype, where labelled cells arising from 1/16 injection of *tbx2b* MO were excluded from the neural plate (as defined by *sox19* expression) at 10 hpf, was significantly reduced in a dose-dependent manner by co-injection of a *tbx2b* mRNA lacking the target site for *tbx2b* MO. This phenomenon was accompanied by the appearance of labelled cells in the midline and the notochord at 10 and 24 hpf, respectively, in about 10% of experimental embryos (Fig. 3E). In all, the results support the specificity of *tbx2b* MO and demonstrate the early requirement of Tbx2b in the formation of the neural plate.

The 'exclusion' phenotype points to aberrant cell migration within the embryonic ectoderm, suggesting that cell adhesion could be compromised. The surface of embryos undergoing gastrulation is smooth (Fig. 4A). By contrast, pan-embryonic injections of *tbx2b* MO (Fig. 4B) caused rounding of cells on the surface of morphants. As a result, the morphants acquired a 'rough' phenotype, suggesting that cell adhesion in vivo was affected. Currently, we do not know if there were other cell polarity defects associated with this 'rough' phenotype.

To test whether Tbx2b-depleted cells exhibited altered cell adhesion properties, cell re-association experiments were performed. Texas Red-labelled animal caps of 5 hpf embryos from wild-type or MO-depleted embryos were dissociated and mixed with fluorescein-labelled wild-type cells and cultured as hanging-drop. After 24 hours, the two control-derived populations formed a single aggregate (Fig. 4D), suggesting similar surface adhesion properties. By contrast, cells that were co-injected with fluorescein and *tbx2b* MO (Fig. 4E) formed shells around small aggregates of control cells. This is consistent with idea that aggregated control cells have higher level of the same cadherin than do morphant cells in the outer shells (Steinberg and Takeichi, 1994).

Cadherins are essential for cell adhesion. Indeed, supporting the observation from hanging-drop culture, the level of cadherins failed to increase during gastrulation in *tbx2b* morphants (Fig. 4G). This suggests that the deficiency in cadherins could be the proximal cause of the defects in cell adhesion and migration observed in vivo. It is known that during epiboly, cell-cell adhesion plays a crucial role in maintaining the integrity of the ectodermal sheet (Concha and Adams, 1998). Although *Xbra* is known to inhibit cell migration, it was shown to do so by inhibiting adhesion to fibronectin instead of affecting the level of cadherin directly (Kwan and Kirschner, 2003). The mutation in *parachute* (*pac*) eliminates N-cadherin. Similar to *tbx2b* morphants, this mutant is characterized by abnormal anterior neural tube (Lele et al., 2002). Indeed, cells transplanted from $pac^{-/-}$ into wild-type hosts failed to populate the anterior CNS by 24 hpf (9/9). By contrast, cells from heterozygous siblings were found in the CNS of hosts (10/10).

To demonstrate that migration of cells deficient in Tbx2 is also affected, morphant cells were co-transplanted with control cells into the ectoderm of wild-type embryos and observed in vivo (Fig. 4H-I). The morphant cells lagged behind control cells when migrating to the dorsal side of the embryo at 50% (Fig. 4J) and 80% epiboly (not shown). In addition, by the end of gastrulation, these cells did not express *sox19* and remained outside the neural plate at 10 hpf (Fig. 4L). Thus, an essential aspect of neural plate formation is the requirement of Tbx2b for optimal cell adhesion and consequent cell movement into the dorsal ectoderm destined to develop as the neural plate.

The appearance of 'exclusion' phenotype from 1/16 injection of *tbx2b* MO in neural plate stage embryos provided a quick assay to screen for genes that are potentially functioning in the same pathway as *tbx2b* (Table 1). Reagents (MOs or mRNAs) were injected in the 1/16 manner together with a fluorescein tracer, and the number of embryos exhibiting the 'exclusion' phenotype at 10 hpf was scored. A percentage similar to or higher than that obtained from *tbx2b* MO suggests a potential correlation of function. MOs and mRNAs used in the screen were previously tested in pan-embryonic injections

for efficacy and viability (data not shown). Where available, MOs were tested to phenocopy the respective mutants (see Materials and methods). The assay allowed us to narrow down quickly on a potential pathway.

Consistent with the role of Bmp suppression in neural induction, 1/16 injection of *bmp2* mRNA led to 'exclusion' phenotype in all experimental embryos. This is in contrast to injection of dn-BmpR, which blocked Bmp signalling (Neave et al., 1997). A 1/16 injection of *b-jun* and *c-jun*, known to be involved in CE movement through non-canonical Wnt signalling (Myers et al., 2002), led to complete exclusion, supporting the notion that the 'exclusion' phenotype arises from a cell movement defect. A 1/16 injection of PKA (Fig. 4N, a negative regulator of the Hh pathway) (Hammerschmidt et al., 1997) and XFD (Fig. 4O, which blocked FGF signalling) (Schulte-Merker et al., 1995) failed to recapitulate the exclusion phenotype and thus ruled out the involvement of the Hedgehog and FGF pathways upstream of Tbx2b. By contrast, interference of Wnt signalling by overexpression of a dn-Fz7 that lacked the C-terminal intracellular PDZ-binding domain led to the 'exclusion' phenotype (Fig. 4P). Detailed analyses showed that a similar effect could be obtained with anti-*fz7* MO (*fz7* MO, Fig. 4Q), but not with MOs against the closely related *fz7a* and the more distantly related *fz2* (Table 1).

Next, intracellular components downstream of Fz7 were analyzed (Table 1). Dishevelled (Ds) consists of three functional domains: the DIX domain is essential for β-catenin activity, whereas the PDZ and DEP domains are involved in non-canonical signalling (Topczewski et al., 2001). Constructs of *Xenopus* Ds (Xds) with domain deletions were injected in the 1/16 manner. Of these three constructs, only XdsΔDIX, which lacks DIX domain, phenocopied the exclusion phenotype, suggesting that a disruption of β-catenin signalling could contribute into the 'exclusion' phenotype. Indeed, TOP-flash assay of Fz7 morphant embryos indicated a marked decrease in the level of β-catenin-dependent Tcf activity (Fig. 5A). Although MOs against *b-jun* and *c-jun* led to exclusion, the inability of the XdsΔDEP (without DEP domain) and XdsΔPDZ (without PDZ domain) to induce exclusion is particularly interesting as the non-canonical pathway is known to function via corresponding domains to activate the JNK/SAPK cascade (Korinek et al., 1997). Owing to the pleiotropic nature of β-catenin and Jun, rescue experiments with *tbx2b* remain complicated. In summary, the screen showed that interfering with Wnt signalling consistently produced the same effect as depletion of Tbx2. These results led us to focus our analysis on *fz7*.

fz7 is expressed in the ectoderm during gastrulation (Fig. 5B); thus, it is present in the ectodermal cells at the time when they acquire neural fates. Ectopic overexpression (by intracellular injection of DNA construct into one-cell stage embryos) of a dn-Fz7-EGFP/BAC (with the EGFP inserted into the C terminus to replace the stop codon) caused the loss of *tbx2b* expression (Fig. 5C). Real-time PCR analysis of *tbx2b*- and *fz7*-morphants (MOs injected at 0.5 pmol and 0.2 pmol)

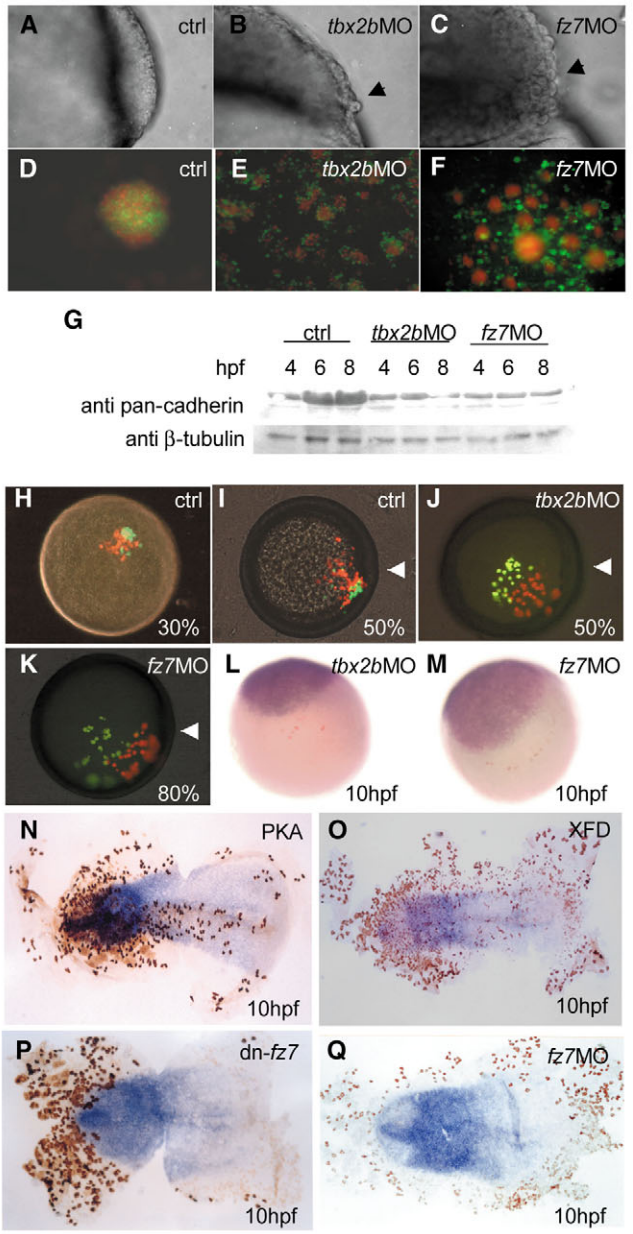

Fig. 4. (A-G) Early function of Tbx2b and Fz7 is required for cell adhesion. The smooth surface of (A) a wild-type gastrulating embryo, is in contrast to the 'rough phenotype' (black arrows) in (B) Tbx2b and (C) Fz7 morphants. (D) In control, dissociated 6 hpf cells labelled with fluorescein (green) and Texas Red (red) formed a single aggregate after 24 hours in hanging drop culture. By contrast, cells derived from fluorescein-labelled (E) Tbx2b- and (F) Fz7-morphant cells formed single layer shells around wild-type Texas Red-labelled aggregates. (G) Western blot with a pan-cadherin antibody showed that the level of cadherins in Tbx2b and Fz7 morphants remained the same or declined in contrast to the control. (H-M) Cell movement during gastrulation was affected in Fz7- or Tbx2b-deficient cells. Control cells with fluorescein and Texas Red transplanted into wild-type host at (H) 30% epiboly co-migrated towards the dorsal side by (I) 50% epiboly, but fluorescein labelled (J) Tbx2b and (K) Fz7 morphant cells were unable to migrate (white arrowheads indicate position of the shield). A 10 hpf embryo stained for fluorescein (brown) shows that transplanted (L) Tbx2b and (M) Fz7 morphant cells were excluded from the *sox19*-positive neural plate. (N-Q) Flat mounts of 10 hpf embryos, double stained for fluorescein (brown) and *sox19* (blue), after single cell injection at 16-cell stage with (N) PKA, (O) XFD, (P) dn-Fz7 and (Q) *fz7* MO.

Table 1. Screen shows the involvement of Fz7 and the Wnt pathway in the 'exclusion' phenotype

Reagent	Embryos with phenotype (%)	*n*
Control MO	0	50
tbx2b MO	65	38
aa+*tbx2b*	36	22
bmp2	100	26
dn-BMPR	8	25
PKA	0	25
dn-fz7	40	25
*fz7*MO	73	45
aa+*tbx2b*	42	26
*fz7a*MO	7	26
*fz2*MO	22	27
XdsΔDIX	62	26
XdsΔDEP	0	26
XdsΔPDZ	0	23
b-jun MO	100	21
c-jun MO	100	17
stbm MO	0	15
ntl MO	9	34
Pertussis toxin	17	24

showed that whereas *fz7* MO downregulates *fz7* and *tbx2b* transcription at 5 hpf, *tbx2b* MO has no effect on the transcription of *fz7* and its target mRNA (Fig. 5E).

Further analysis showed that *fz7* morphants displayed 'rough' phenotype during gastrulation (Fig. 4C), *fz7*-deficient cells failed to aggregate with control cells in hanging-drop cultures (Fig. 4F), *fz7* morphants failed to upregulate cadherins (Fig. 4G), and transplanted *fz7*-deficient cells did not co-migrate with control cells (Fig. 4K,M). A 1/16 co-injection of *tbx2b* mRNA with *fz7* MO led to the appearance of morphologically undifferentiated labelled cells in the eyes and forebrain at 24 hpf (Fig. 5D), suggesting that Tbx2b is able to rescue the cell movement, but not the fate specification function of Fz7. Owing to the pleiotropic nature of Fz7 function, attempts to rescue the 'exclusion' phenotype of *fz7* MO by co-injection of a *fz7* mRNA without the MO target site were unsuccessful. Together, these results suggest that Tbx2b may function as a downstream effector of Fz7-mediated cell movement during neural plate formation (Djiane et al., 2000).

Is the cell movement defect arising from Tbx2b 'knockdown' the direct cause of neuronal specification failure in these cells later in development? To answer this, cells from shield stage (6 hpf) of Tbx2b morphant donors were transplanted directly into the dorsal side of homochronic wild-type hosts at two locations: one that gives rise to the eyes and the other to the hindbrain by 24 hpf (Kimmel et al., 1990; Moens and Fritz, 1999). Whereas wild-type cells transplanted into wild-type hosts ended up in appropriate positions and differentiated according to neighbouring tissues (Fig. 5F-G), in both cases all transplanted morphant cells ended up in the intended locations at 24 hpf but could not acquire the typical morphology of cells in these tissues, suggesting that they were unable to differentiate properly (not shown).

However, owing to the delay in the onset and progression of gastrulation in morphants, the donors were not morphologically equivalent to wild-type shield stage embryos (they resembled 4 hpf embryos). To confirm that the failure in specification was not due to the delay in development, transplantation was repeated with cells from morphant donors at shield stage irrespective of the actual age (~8 hpf). Although

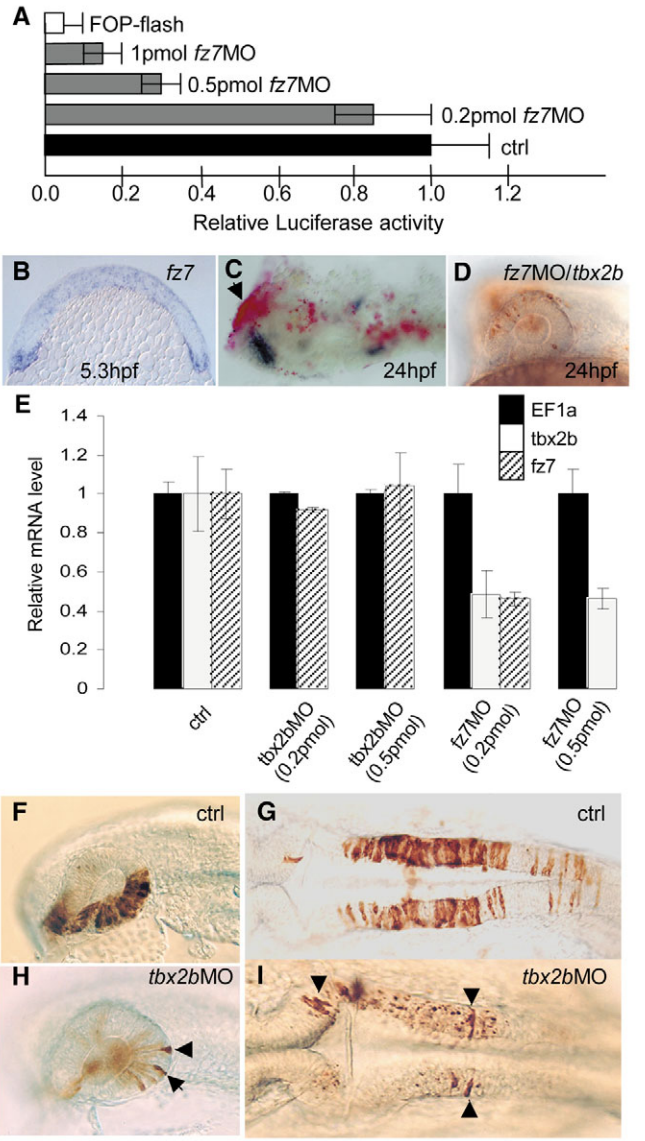

Fig. 5. (A-D) Tbx2b is regulated by Fz7. (A) TOP-flash assay shows a reduction of β-catenin-dependent Tcf activity in *fz7* morphants. (B) Expression of *fz7* at 5.3 hpf (cross-section). (C) Expression of a dn-fz7-EGFP/BAC (red, see Materials and methods) caused the loss of *tbx2b* expression (blue) in the eye (arrow). (D) The absence of *fz7* MO/fluorescein-injected cells in the eyes and CNS at 24 hpf is rescued by co-injection of *tbx2b* mRNA. (E) Real-time PCR analysis of Tbx2b and Fz7 morphants showed a decrease in *tbx2b* and *fz7* transcripts in the presence of *fz7* MO, but no effect from *tbx2b* MO at 5 hpf. *n*=15 for control, *n*=7 for *tbx2b* MO and *n*=4 for *fz7* MO. (F-I) Rescue of cell movement defect by transplantation into wild-type host at shield stage. Wild-type donor cells differentiated into morphologically distinct cells in the eye (F) and hindbrain (G) by 24 hpf. By contrast, only a few Tbx2b-deficient cells differentiated into distinct eye (H) and hindbrain (I) cells (arrowheads).

a few transplanted cells managed to regain the typical morphology of cells in these tissues (arrowheads, Fig. 5H,I), the majority did not. This result suggests that Tbx2b may have a later role in neuronal differentiation. Similarly, we demonstrated that in the absence of Fz7, overexpression of *tbx2b* could only rescue the cell movement defect but not the

subsequent differentiation of transplanted cells (Fig. 5D). Altogether, these results suggest that, independent of its requirement in cell adhesion and cell movement, Tbx2b is necessary, but insufficient, for neuronal differentiation in the late neuroectoderm. *tbx2b* is expressed at high levels in sensory cells and other neuronal lineages later in development, and is therefore likely to play a role in their differentiation (Dheen et al., 1999).

Discussion

The previous loss-of-function study using dn-Tbx2b has shown a role for Tbx2b in the notochord (Dheen et al., 1999). In this study, we used morpholino antisense oligos (MO) to effect a 'knockdown' of Tbx2b to address its early function in development suggested by the presence of its transcripts as early as 50% epiboly, before they were detected by whole-mount in situ hybridization. The specificity of the MO used was established by its ability to block translation of myc-tagged Tbx2b and produce comparable phenotypes in the notochord demonstrated with dn-Tbx2b.

Pan-embryonic injection of *tbx2b* MO led to a delay in epiboly and malformed anterior forebrain at 24 hpf. In order to separate analyses in ectoderm from mesoderm, we focused on the behaviour of Tbx2b-depleted ectodermal cells in an otherwise normal wild-type embryo. We demonstrated that cells deficient in Tbx2b were consistently excluded from the neural plate at 10 hpf, and did not develop as neural cells by 24 hpf. Embryonic cells are pluripotent up to the early gastrula stages (Ho and Kimmel, 1993). Therefore, alteration of cell movement can cause changes in fate specification by virtue of exposure to local signalling cues prevalent in the 'adopted' position. Conversely, a failure in fate specification can cause a change in cell movement behaviour. Either mechanism could lead to exclusion of cells from the neural plate. However, analysis of expression of *bmp2*, *fz7* and *sox19* suggest that early fate specification is not affected by 'knockdown' of Tbx2b. Indeed, the neural plate is induced in the Tbx2b morphant. Our results thus indicate that Tbx2b functions in cell migration in the ectoderm during the formation of the neural plate.

It has been shown that strong intercellular adhesion plays a crucial role in maintaining the integrity of the gastrulating ectodermal sheet (Concha and Adams, 1998). In zebrafish null mutant for N-cadherin (*pac*), neuroectodermal cell adhesion is altered, leading to compromised convergent cell movements during neurulation (Lele et al., 2002). We show that cells depleted of Tbx2b have reduced cadherins, and this altered cell adhesion is likely to be the cause of migration defects leading to their exclusion from the neural plate in chimeras. As β-catenin binds tightly to the cytoplasmic domain of type 1 cadherins (Jamora et al., 2003), loss of cadherins in Tbx2b-depleted cells may lead to defects in β-catenin stabilization and localization, with subsequent consequences in differentiation. As such, there is a possible convergence of Tbx2b, Wnt, β-catenin and cadherin signalling in adhesion, morphogenetic movement and differentiation.

Although *spt* (Ho and Kane, 1990), *T* (Wilson and Beddington, 1997), *ntl* (Conlon and Smith, 1999) and *Tbx5* (Hatcher et al., 2004) have been implicated in cell movement, the roles demonstrated for them are confined within the context of mesoderm. Still, these studies showed that in chimeras with neighbouring wild-type and T-box-deficient cells, the movement of wild-type cells in their normal developmental context resulted in the exclusion of T-box-deficient cells similar to what we demonstrate here. It would seem that this is a common phenomenon and may indicate a general functional mechanism for T-box proteins in cell migration during development.

Interestingly, overexpression of Tbx2b in the ectoderm led to the appearance of cells in the notochord, a mesodermal structure. Although it is known that Tbx2b is required for the specification of axial mesodermal structures at the expense of lateral mesodermal tissues (Dheen et al., 1999), what we demonstrate here is its ability to transfate cells from ectoderm to dorsal mesoderm. We do not yet know the precise mechanism of this phenomenon. However, we show here that a low level of Tbx2b is needed for proper cell adhesion and cell movement within the ectodermal sheet. It is possible that dorsal mesoderm has higher levels of cell adhesion, and the affected cells move into the underlying mesoderm during gastrulation. Analysis with maternal-zygotic *one-eyed-pinhead* (MZ*oep*) mutant cells showed that internalization and mesendoderm formation in zebrafish can be attained autonomously by single cells (Carmany-Rampey and Schier, 2001). If so, it opens the possibility that differential activation of Tbx2b is a mechanism by which systematic differences in cell surface properties and cell segregation behaviour is modulated for the purpose of long-term effects on cell fate specification. More analysis is needed to better understand this observation.

The exclusion phenotype provided a rapid assay for screening signalling pathways that Tbx2b might be operating within. The screen suggests that Tbx2b functions within the context of Wnt signalling, specifically through the receptor Fz7. Zebrafish Fz7, like its homologue in *Xenopus*, has a broad range of functions from fate specification to cell movement, but it is the cell movement requirement for Fz7 that is mediated by Tbx2b. As *Drosophila* Omb also acts within the Wnt context in multiple developmental situations (Grimm and Pflugfelder, 1996), this developmental link may be conserved in evolution. Although Fz7 is shown to regulate *tbx2b* transcriptionally, a full analysis of the detailed molecular mechanism is beyond the scope of this study. Preliminary analysis of the 2.5 kb 5′ genomic sequence of *tbx2b* identified numerous Tcf-binding sites (not shown), hinting at the possibility of regulation of *tbx2b* transcription *via* β-catenin/Tcf.

The functional roles of the canonical and non-canonical Wnt pathways were thought to be quite different (Moon et al., 1997). In vertebrates, Wnt-dependent morphogenetic cell movements were linked to the non-canonical pathway (Tada et al., 2000; Heisenberg et al., 2000), which directly controls Ds-mediated cell polarity (Wallingford et al., 2000). The canonical Wnt pathway was associated with the initiation of CE movements, but not movement per se (Moon et al., 1997). Although β-catenin acts in both signalling and adhesion in insects and vertebrates (Moon et al., 2002), the involvement of the canonical Wnt pathway in cell movement has been shown only in invertebrates (Korswagen, 2002).

In the *Xenopus* blastula, β-catenin was proposed to regulate CE and mediate cell fate via two parallel pathways involving Nodal-related 3 and Siamois, respectively (Kuhl et al., 2001).

In zebrafish, β-catenin modulates Nodal signalling, to regulate both cell fate and cell movement (Myers et al., 2002); and *Boz*, to repress *bmp2b* (Leung et al., 2003). In this study, the ability of Fz7 to mediate Wnt signalling via the DIX-domain of Ds to effect cell adhesion and cell movement during gastrulation suggests that Ds may not function in a strictly modular manner. The current notion that cell movement events are mediated by the non-canonical pathway through the DEP- and PDZ-domains of Ds may need to be looked at afresh.

It has been shown recently that Tbx2 is required for patterning the atrioventricular canal and for morphogenesis of the outflow tract during heart development in mice (Harrelson et al., 2004). Cell migration plays an important role in heart formation in teleosts (Glickman and Yelon, 2002) and amniotes (Hatcher et al., 2004). Although *tbx2b* is expressed in the developing heart and the morphants display cardiac defects later in development (not shown), it remains to be seen if Tbx2b plays a role in the migration of cardiac cells.

Authors are indebted to members of V.K.'s laboratory, to W. Chia and to P. Singh for critical reading of this manuscript. We thank R. Moon, S. Vriz and U. Takeda for reagents and cDNA. We also thank W. Chia, S. H. Yang, E. Manser, D. Grunwald, C.-P. Heisenberg and D. Kimelman for discussion. We thank the anonymous reviewers for their invaluable comments that led to improvement of the manuscript. We apologise to many colleagues whose work was not referred to in this publication owing to space limitations. This work was supported by a research grant from the Agency for Science, Technology and Research of Singapore to V.K. Authors declare that they have no competing financial interests.

References

Baker, J., Beddington, R. and Harland, R. (1999). Wnt signaling in *Xenopus* embryos inhibits *Bmp4* expression and activates neural development. *Genes Dev*. **13**, 3149-3159.

Carmany-Rampey, A. and Schier, A. F. (2001). Single-cell internalization during zebrafish gastrulation. *Curr. Biol*. **11**, 1261-1265.

Concha, M. and Adams, R. (1998). Oriented cell divisions and cellular morphogenesis in the zebrafish gastrula and neurula: a time-lapse analysis. *Development* **125**, 938-994.

Conlon, F. L. and Smith, J. C. (1999). Interference with brachyury function inhibits convergent extension, causes apoptosis, and reveals separate requirements in the FGF and activin signalling pathways. *Dev. Biol*. **213**, 85-100.

Dheen, T., Sleptsova-Friedrich, I., Xu, Y., Clark, M., Lehrach, H., Gong, Z. and Korzh, V. (1999). Zebrafish tbx-c functions during formation of midline structures. *Development* **126**, 2703-2713.

Djiane, A., Riou, J., Umbhauer, M., Boucaut, J. and Shi, D. (2000). Role of frizzled 7 in the regulation of convergent extension movements during gastrulation in Xenopus laevis. *Development* **127**, 3091-3100.

Fekany-Lee, K., Gonzalez, E., Miller-Bertoglio, V. and Solnica-Krezel, L. (2000). The homeobox gene bozozok promotes anterior neuroectoderm formation in zebrafish through negative regulation of BMP2/4 and Wnt pathways. *Development* **127**, 2333-2345.

Glickman, N. S. and Yelon, D. (2002). Cardiac development in zebrafish: coordination of form and function. *Semin. Cell Dev. Biol.* **13**, 507-513.

Grimm, S. and Pflugfelder, G. O. (1996). Control of the gene optomotor-blind in Drosophila wing development by decapentaplegic and wingless. *Science* **271**, 1601-1604.

Hammerschmidt, M., Bitgood, M. and McMahon, A. P. (1997). Protein kinase A is a common negative regulator of hedgehog signalling in the vertebrate embryo. *Genes Dev.* **10**, 647-658.

Hatcher, C. J., Diman, N. Y., Kim, M. S., Pennisi, D., Song, Y., Goldstein, M. M., Mikawa, T. and Basson, C. T. (2004). A role for Tbx5 in proepicardial cell migration during cardiogenesis. *Physiol. Genomics* **18**, 129-140.

Harrelson, Z., Kelly, R. G., Goldin, S. N., Gibson-Brown, J. J., Bollag, R. J., Silver, L. M. and Papaioannou, V. E. (2004). Tbx2 is essential for patterning the atrioventricular canal and for morphogenesis of the outflow tract during heart development. *Development* **131**, 5041-5052.

Heisenberg, C. P., Tada, M., Rauch, G. J., Saude, L., Concha, M. L., Geisler, R., Stemple, D. L., Smith, J. C. and Wilson, S. W. (2000). Silberblick/Wnt11 mediates convergent extension movements during zebrafish gastrulation. *Nature* **405**, 76-81.

Ho, R. K. and Kane, D. A. (1990). Cell-autonomous action of zebrafish spt-1 mutation in specific mesodermal precursors. *Nature* **348**, 728-730.

Ho, R. K. and Kimmel, C. B. (1993). Commitment of cell fate in the early zebrafish embryo. *Science* **261**, 109-111.

Jacobs, J. J., Keblusek, P., Robanus-Maandag, E., Kristel, P., Lingbeek, M., Nederlof, P. M., van Welsem, T., van de Vijver, M. J., Koh, E. Y., Daley, G. Q. et al. (2000). Senescence bypass screen identifies TBX2, which represses Cdkn2a(p19ARF) and is amplified in a subset of human breast cancers. *Nat. Genet.* **26**, 291-299.

Jamora, C., DasGupta, R., Kocieniewski, P. and Fuchs, E. (2003). Links between signal transduction, transcription and adhesion in epithelial bud development. *Nature* **422**, 317-322.

Kimmel, C. B., Warga, R. M. and Schilling, T. M. (1990). Origin and organization of the zebrafish fate map. *Development* **108**, 581-594.

Kopp, A. and Duncan, I. (1997). Control of cell fate and polarity in the adult abdominal segments of Drosophila by optomotor-blind. *Development* **124**, 3715-3726.

Korinek, V., Barker, N., Morin, P. J., van Wichen, D., de Weger, R., Kinzler, K. W., Vogelstein, B. and Clevers, H. (1997). Constitutive transcriptional activation by a beta-catenin-Tcf complex in APC–/– colon carcinoma. *Science* **275**, 1784-1787.

Korswagen, H. C. (2002). Canonical and non-canonical Wnt signaling pathways in Caenorhabditis elegans: variations on a common signaling theme. *BioEssays* **24**, 801-810.

Kuhl, M., Geis, K., Sheldahl, L. C., Pukrop, T., Moon, R. T. and Wedlich, D. (2001). Antagonistic regulation of convergent extension movements in *Xenopus* by Wnt/beta-catenin and Wnt/Ca(2+) signaling. *Mech. Dev*. **106**, 61-76.

Kwan, K. M. and Kirschner, M. W. (2003). *Xbra* functions as a switch between cell migration and convergent extention in the *Xenopus* gastrula. *Development* **130**, 1961-1972.

Larue, L., Antos, C., Butz, S., Huber, O., Delmas, V., Dominis, M. and Kemler, R. (1996). A role for cadherins in tissue formation. *Development* **122**, 3185-3194.

Lele, Z., Folchert, A., Concha, M., Rauch, G. J., Geisler, R., Rosa, F., Wilson, S. W., Hammerschmidt, M. and Bally-Cuif, L. (2002). parachute/n-cadherin is required for morphogenesis and maintained integrity of the zebrafish neural tube. *Development* **129**, 3281-3294.

Leung, T., Bischof, J., Soll, I., Niessing, D., Zhang, D., Ma, J., Jackle, H. and Driever, W. (2003). bozozok directly represses bmp2b transcription and mediates the earliest dorsoventral asymmetry of bmp2b expression. *Development* **130**, 3639-3649.

Marlow, F., Gonzalez, E. M., Yin, C., Rojo, C. and Solnica-Krezel, L. (2004). No tail co-operates with non-canonical Wnt signaling to regulate posterior body morphogenesis in zebrafish. *Development* **131**, 203-216.

Moens, C. B. and Fritz, A. (1999). Techniques in neural development. *Methods Cell Biol*. **59**, 253-272.

Moon, R. T., Brown, J. D. and Torres, M. (1997). WNTs modulate cell fate and behaviour during vertebrate development. *Trends Genet.* **13**, 157-162.

Moon, R. T., Bowerman, B., Boutros, M. and Perrimon, N. (2002). The promise and perils of Wnt signaling through beta-catenin. *Science* **296**, 1644-1646.

Munoz-Sanjuan, I. and Brivanlou, A. H. (2002). Neural induction, the default model and embryonic stem cells. *Nat. Rev. Neurosci*. **3**, 271-280.

Myers, D. C., Sepich, D. S. and Solnica-Krezel, L. (2002). Convergence and extension in vertebrate gastrulae: cell movements according to or in search of identity? *Trends Genet.* **18**, 447-455.

Narayanan, K., Williamson, R., Zhang, Y., Stewart, A. F. and Ioannou, P. A. (1999). Efficient and precise engineering of a 200 kb beta-globin human/bacterial artificial chromosome in E. coli DH10B using an inducible homologous recombination system. *Gene Ther.* **6**, 442-447.

Nasevicius, A. and Ekker, S. C. (2000). Effective targeted gene 'knockdown' in zebrafish. *Nat. Genet*. **26**, 216-220.

Neave, B., Holder, N. and Patient, R. (1997). A graded response to BMP-4 spatially coordinates patterning of the mesoderm and ectoderm in the zebrafish. *Mech. Dev*. **62**, 183-195.

Nelson, W. J. and Nusse, R. (2004). Convergence of Wnt, beta-catenin, and cadherin pathways. *Science* **303**, 1483-1487.

Packham, E. A. and Brook, J. D. (2003). T-box genes in human disorders. *Hum. Mol. Genet.* **12**, R37-R44.
Park, M. and Moon, R. T. (2002). The planar cell-polarity gene stbm regulates cell behaviour and cell fate in vertebrate embryos. *Nat. Cell Biol.* **4**, 20-25.
Prince, S., Carreira, S., Vance, K. W., Abrahams, A. and Goding, C. R. (2004). Tbx2 directly represses the expression of the p21 WAF1 cyclin-dependent kinase inhibitor. *Cancer Res.* **64**, 1669–1674.
Schulte-Merker, S. and Smith, J. C. (1995). Mesoderm formation in response to Brachyury requires FGF signalling. *Curr. Biol.* **5**, 62-67.
Shih, J. and Keller, R. (1994). Gastrulation in Xenopus laevis: involution – a current view. *Semin. Dev. Biol.* **5**, 85-90.
Smith, J. (1999). T-box genes: what they do and how they do it. *Trends Genet.* **15**, 154-158.
Steinberg, M. S. and Takeichi, M. (1994). Experimental specification of cell sorting, tissue spreading, and specific spatial patterning by quantitative differences in cadherin expression. *Proc. Natl. Acad. Sci. USA* **91**, 206-209.
Suzuki, T., Takeuchi, J., Koshiba-Takeuchi, K. and Ogura, T. (2004). Tbx genes specify posterior digit identity through Shh and BMP signaling. *Dev. Cell* **6**, 43-53.
Takabatake, Y., Takabatake, T., Sasagawa, S. and Takeshima, K. (2002). Conserved expression control and shared activity between cognate T-box genes Tbx2 and Tbx3 in connection with Sonic hedgehog signaling during Xenopus eye development. *Dev. Growth Differ.* **44**, 257-271.
Tada, M. and Smith, J. C. (2000). Xwnt11 is a target of Xenopus Brachyury: regulation of gastrulation movements *via* Dishevelled, but not through the canonical Wnt pathway. *Development* **127**, 2227-2238.
Topczewski, J., Sepich, D. S., Myers, D. C., Walker, C., Amores, A., Lele, Z., Hammerschmidt, M., Postlethwait, J. and Solnica-Krezel, L. (2001). The zebrafish glypican knypek controls cell polarity during gastrulation movements of convergent extension. *Dev. Cell* **1**, 251-264.
Vriz, S. and Lovell-Badge, R. (1995). The zebrafish Zf-Sox 19 protein: a novel member of the Sox family which reveals highly conserved motifs outside of the DNA-binding domain. *Gene* **153**, 275-276.
Wallingford, J. B., Rowning, B. A., Vogeli, K. M., Rothbacher, U., Fraser, S. E., Harland, R. M. (2000). Dishevelled controls cell polarity during Xenopus gastrulation. *Nature* **405**, 81-85.
Wessely, O., Agius, E., Oelgeschlager, M., Pera, E. M. and De Robertis, E. M. (2001). Neural induction in the absence of mesoderm: b-catenin-dependent expression of secreted BMP antagonists at the blastula stage in Xenopus. *Dev. Biol.* **234**, 161-173.
Wilson, V. and Beddington, R. (1997). Expression of T protein in the primitive streak is necessary and sufficient for posterior mesoderm movement and somite differentiation. *Dev. Biol.* **192**, 45-58.
Wilson, V. and Conlon, F. (2002). The T-Box family. *Genome Biol.* **3**, 3008.1-3008.7.